

# Energy exchange between two orthogonally polarized waves by cascading of two quasi-phase-matched quadratic processes

Benjamin F. Johnston<sup>1\*</sup>, Peter Dekker<sup>1</sup>, Solomon M. Saltiel<sup>2†</sup>, Yuri S. Kivshar<sup>3‡</sup> and Michael J. Withford<sup>1</sup>

*Centre for Ultrahigh Bandwidth Devices for Optical Systems (CUDOS)*

<sup>1</sup>*Centre for Lasers and Applications, Macquarie University, Sydney, NSW 2109, Australia*

<sup>2</sup>*Faculty of Physics, University of Sofia, 5 J. Bourchier Boulevard, Sofia, BG-1164, Bulgaria*

<sup>3</sup>*Nonlinear Physics Centre, Research School of Physical Sciences and Engineering, Australian National University, Canberra, ACT 0200*

[\\*benjamin@ics.mq.edu.au](mailto:benjamin@ics.mq.edu.au), [†saltiel@phys.uni-sofia.bg](mailto:saltiel@phys.uni-sofia.bg); [‡yvk124@rsphysse.anu.edu.au](mailto:yvk124@rsphysse.anu.edu.au)

**Abstract:** We demonstrate energy exchange between two orthogonally polarized optical waves as a consequence of a two-color multistep parametric interaction. The energy exchange results from cascading of two quasi-phase-matched (QPM) second-harmonic parametric processes, and it is intrinsically instantaneous. The effect is observed when both the type-I (*ooe*) second-harmonic generation process and higher QPM order type-0 (*eee*) second-harmonic generation processes are phase-matched simultaneously in a congruent periodically-poled lithium niobate crystal. The two second-harmonic generation processes share a common second-harmonic wave which couple the two cross-polarized fundamental components and facilitate an energy flow between them. We demonstrate a good agreement between the experimental data and the results of numerical simulations.

©2007 Optical Society of America

OCIS codes: (190.4360) Nonlinear optics, devices

---

## References and links

1. M. H. Chou, K. R. Parameswaran, and M. M. Fejer, "Multiple-channel wavelength conversion by use of engineered quasi-phase-matching," *Opt. Lett.* **24**, 1157-1159 (1999).
2. S. Zhu, Y. Zhu, and N. Ming, "Quasi-phase-matched third-harmonic generation in a quasi-periodic optical superlattice," *Science* **278**, 843-846 (1997).
3. A. H. Norton and C. M. de Sterke, "Aperiodic one-dimensional structures for quasi-phase matching," *Opt. Express* **12**, 841-846 (2004).
4. N. G. R. Broderick, R. T. Bratfalean, T. M. Monro, D. J. Richardson, and C. M. de Sterke, "Temperature and wavelength tuning of second-, third-, and fourth-harmonic generation in a two-dimensional hexagonally poled nonlinear crystal," *J. Opt. Soc. Am. B* **19**, 2263-2272 (2002).
5. A. Chowdhury, C. Staus, B. F. Boland, T. F. Kuech, and L. McCaughan, "Experimental demonstration of 1535-1555-nm simultaneous optical wavelength interchange with a nonlinear photonic crystal," *Opt. Lett.* **26**, 1353-1355 (2001).
6. B. F. Johnston, P. Dekker, S. M. Saltiel, M. J. Withford, and Yu. S. Kivshar, "Simultaneous phase matching and interference of two second order parametric processes," *Opt. Express* **14**, 11756-11765 (2006).
7. G. Assanto, G. Stegeman, M. Sheik-Bahae, E. Van Stryland, "All optical switching devices based on large nonlinear phase-shifts from second harmonic generation," *App. Phys. Lett.* **62**, 1324-1326 (1993).
8. G. Assanto, I. Torelli, and S. Trillo, "All-optical processing by means of vectorial interactions in 2nd-order cascading - novel approaches," *Opt. Lett.* **19**, 1720-1722 (1994).
9. S. Saltiel and Y. Deyanova, "Polarization switching as a result of cascading to simultaneously phase-matched quadratic processes," *Opt. Lett.* **24**, 1296-1298 (1999).
10. P. Vidakovic, D. J. Lovering, J. A. Levenson, J. Webjrn, and P. S. J. Russell, "Large nonlinear phase shift owing to cascaded  $\chi^{(2)}$  in quasi-phase-matched bulk LiNbO<sub>3</sub>," *Opt. Lett.* **22**, 277-279 (1997).
11. G. G. Gurzadian, V. G. Dmitriev, and D. N. Nikogosian, *Handbook of Nonlinear Optical Crystals*, 3rd ed., Vol. 64 of Springer Series in Optical Sciences (Springer-Verlag, New York, 1999).

12. M. Reich, F. Korte, C. Fallnich, H. Welling, and A. Tunnermann, "Electrode geometries for periodic poling of ferroelectric materials," *Opt. Lett.* **23**, 1817-1819 (1998).
13. B. F. Johnston and M. J. Withford, "Dynamics of domain inversion in LiNbO<sub>3</sub> poled using topographic electrode geometries," *Appl. Phys. Lett.* **86**, 262901 (2005).
14. L. E. Myers, R. C. Eckardt, M. M. Fejer, R. L. Byer, W. R. Bosenberg, and J. W. Pierce, "Quasi-phase-matched optical parametric oscillators in bulk periodically poled LiNbO<sub>3</sub>," *J. Opt. Soc. Am. B* **12**, 2102-2116 (1995).
15. S. M. Saltiel, A. A. Sukhorukov, and Yu S Kivshar, "Multistep parametric processes in nonlinear optics," *Prog. Opt.* **47**, 1-73 (2005).
16. R. DeSalvo, D. J. Hagan, M. Sheik-Bahae, G. Stegeman, E. W. Van Stryland, and H. Vanherzeele, "Self-focusing and self-defocusing by cascaded 2nd-order effects in KTP," *Opt. Lett.* **17**, 28-30 (1992).
17. G. I. Petrov, O. Albert, J. Etchepare, and S. M. Saltiel, "Cross-polarized wave generation by effective cubic nonlinear optical interaction," *Opt. Lett.* **26**, 355-357 (2001).
18. Y. Sheng, J. Dou, B. Ma, B. Cheng, and D. Zhang, "Broadband efficient second harmonic generation in media with a short-range order," *Appl. Phys. Lett.* **91**, 011101 (2007).
19. P. Yeh, "Photorefractive two-beam coupling in cubic crystals," *J. Opt. Soc. Am. B*, **4**, 1382-1386 (1987).

## 1. Introduction

Cascading of quadratic (or  $\chi^{(2)}$ ) nonlinear parametric optical processes is of fundamental interest for the study of parametric interactions in optics, and can also be used for all-optical processing applications. Of particular interest are nonlinear phase shifts and induced Kerr-like nonlinearities, as well as multi-step frequency conversion. Second-harmonic generation (SHG) or sum-frequency generation (SFG), cascaded with difference-frequency generation (DFG) in periodically poled lithium niobate (PPLN) waveguides has been widely reported as a means for frequency conversion of c-band optical channels in a high-bit-rate low noise fashion, as well as optical gating of signals. Efficient third- and fourth-harmonic generation by cascaded quasi-phase-matching (QPM) has also been demonstrated for generation of visible wavelengths from near and mid IR sources. Most of these applications require the design and fabrication of longitudinal varying QPM gratings, such as phase-reversed [1], Fibonacci [2], other aperiodic one dimensional structures [3] and two dimensional periodically poled structures [4, 5]. We have previously reported simultaneous phase-matching and internal interference of two different types of SHG processes which involve the fundamental waves with equivalent wavelengths but orthogonal polarizations in a single periodic PPLN crystal [6].

In this paper, we demonstrate that such an approach leads to the cascading of SHG and difference frequency mixing (DFM), resulting in the exchange of energy between the fundamental fields. This phenomenon may have applications in single-frequency signal regeneration as the nonlinear transfer function depends on two second-order processes. Other phenomena that may arise from such cascaded interactions have been studied theoretically by several authors, and applications in all-optical amplitude modulation and switching have been suggested [7, 8]. We present a proof of principle based on SHG and subsequent down conversion of a 1064.5 nm Nd: GdVO<sub>4</sub> laser using simultaneous phase-matching of type-0 (ee) and type-I (ooe) SHG in PPLN, in a slightly modified version of the regime suggested in [9]. While large phase shifts have been shown to result from cascading interactions in first-order QPM PPLN [10], the results we present here demonstrate that for the simultaneous QPM of type-0 and type-I processes, an energy exchange between the orthogonal polarization components takes place, which is indicative of an equivalent cubic ( $\chi^{(3)}$ ) process. We also show numerically that an enhancement of the nonlinear phase shift due to cascading of simultaneously phase-matched processes can occur.

## 2. Crystal design and fabrication techniques

Whilst most PPLN crystals are designed for type-0 (eee) parametric mixing to take advantage of the large  $d_{33}$  nonlinear coefficient of lithium niobate, the type-I (ooe) process (with the relevant component  $d_{31}$ ) can also be quasi-phase-matched with reasonable efficiency. The dispersion characteristics in congruent lithium niobate are such that we can simultaneously quasi-phase-match a first-order type-I SHG, with a higher order type-0 SHG, from a 1064 nm (or potentially a 1550 nm) laser source. This can be achieved across a range of processes in

single period QPM crystals by matching the periods of various QPM orders at appropriate temperatures and wavelengths. Figure 1 shows the required poling periods in relation to crystal temperature for SHG from a 1064 nm source on the 5<sup>th</sup> and 7<sup>th</sup> order type-0 QPM, plotted with the periods for the SHG of the first order type-I QPM. Sellmeier relations have been taken from Ref. [11]. The points of interest are the crossing points of the type-0 and type-I periods, where simultaneous QPM can be achieved. In this paper the 7<sup>th</sup> order type-0 process has been targeted, coincident with the 1<sup>st</sup> order type-I process, as the temperature and period required are more convenient for both fabrication and operation. This is due to a more precise fabrication of the longer period crystal, along with temperatures which serve to reduce photorefractive effects but are not so high as to become problematic when seeking to stabilize in ambient room conditions. In addition the two processes will also share a very similar effective nonlinear coefficient. For common values of the coefficients  $d_{33}$  and  $d_{31}$ , the ratio of the nonlinearities for the 1<sup>st</sup> and 7<sup>th</sup> order of the QPM processes is

$$\frac{d_{33}}{7d_{31}} = \frac{27 \text{ pmV}^{-1}}{7 \times 4.7 \text{ pmV}^{-1}} = 0.91. \quad (1)$$

The target fabrication period for the simultaneous phase-matching described above is 45.766  $\mu\text{m}$  at an operating temperature of 452.7 K. The PPLN used for these experiments was poled using topographical electrodes fabricated using laser direct-writing [12,13], followed by electric field poling [14]. Aerotech STA stages with 50 nm positional resolutions were used, allowing PPLN with 45.75  $\mu\text{m}$  period to be produced. Fine angle tuning of the crystal was used to realize the exact required period. The domains were inspected by polishing the z faces of the crystal and viewing under phase contrast microscopy. The slight surface relief ( $\sim 100$  nm) between the different domain orientations produced by polishing is sufficient for detailed viewing of the domains under phase contrast microscopy, without requiring hydrofluoric acid etching. 4.5 mm (100 domains) long crystals were fabricated in 0.5 mm thick congruent lithium niobate. A region of the polished  $-z$  face of a typical crystal produced for these experiments is shown in Fig. 2.

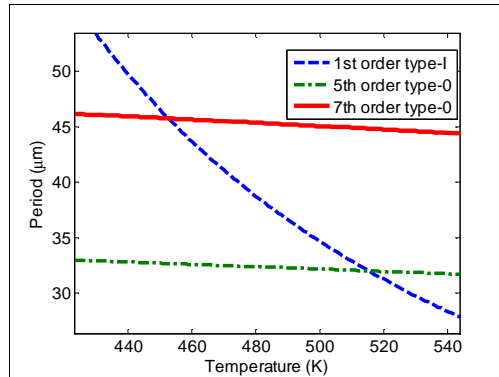


Fig. 1. QPM periods for 1<sup>st</sup> order type-I and 5<sup>th</sup> and 7<sup>th</sup> order type-0 SHG for a 1064 nm fundamental wavelength in lithium niobate as a function of crystal temperature.

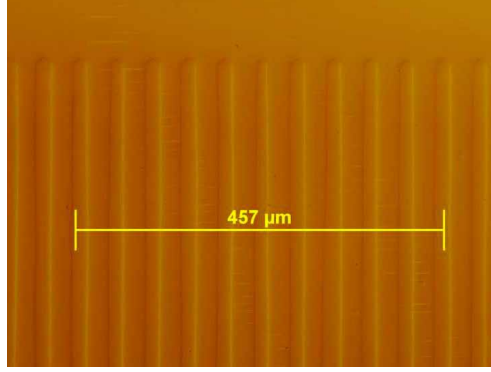


Fig. 2. Domains on the  $-z$  face of a  $45.75 \mu\text{m}$  period PPLN crystals, revealed by polishing and phase-contrast microscopy.

### 3. Two-color parametric cascading: theoretical approach

Two color cascading refers to a class of multistep parametric processes [15] involving just two interacting wavelengths/frequencies but several interacting field components. Two color cascading can result in a number of phenomena including internal interference, nonlinear phase-shifts, polarization rotation and self-phase modulation. In this case we will consider the fundamental and second harmonic fields of the simultaneous phase-matched type-0 and type-I SHG processes described above. While this scenario shares some similarities to the type-II ( $oeo/eoe$ ) process in materials such as KTP, described previously by DeSalvo *et al* [16], this approach is distinct in that we have two discrete phase-matchings, either of which can produce a second harmonic field independently of the other. This is to say that the components of any input polarization state of the fundamental field will be phase-matched by either the type-0 or type-I. This is in contrast to type-II processes where a pure  $e$  or  $o$  wave will not produce a phase-matched second harmonic field. Having two discrete phase-matchings lends itself well to seeding the back conversion process characteristic in two color cascading. The stronger component of the fundamental fields will dominate the generation of the SH field while the weaker component will seed the difference frequency generation on the orthogonal polarization. This cascading of energy from the dominant fundamental field to the second harmonic and then to the orthogonal and weaker fundamental can be represented by the cascading of fields as  $(e_1e_1e_2 \rightarrow e_2o_1o_1)$ , or equivalently by  $(o_1o_1e_2 \rightarrow e_2e_1e_1)$ , which is indicative of an equivalent cubic process,  $(e_1e_1o_1o_1)$  or  $(o_1o_1e_1e_1)$ . This is somewhat analogous to seeded cross-polarized wave generation discussed earlier [17].

A general form of the coupled-field equations describing simultaneously phase-matched SHG with a commonly polarized SH field may be given as,

$$\frac{dA}{dx} = -i\sigma_1 SA^* \exp(-i\Delta k_1 x), \quad (2)$$

$$\frac{dB}{dx} = -i\sigma_2 SB^* \exp(-i\Delta k_0 x), \quad (3)$$

$$\frac{dS}{dx} = -i\sigma_3 AA \exp(i\Delta k_1 x) - i\sigma_4 BB \exp(i\Delta k_0 x), \quad (4)$$

where A, B and S are the complex amplitudes of the two orthogonal fundamental components and second-harmonic respectively,  $\sigma$ 's are the nonlinear constants, encapsulating nonlinear coefficients and impedances, and  $\Delta k_1$  and  $\Delta k_0$ , are the wave vector mismatches of the type-I ( $oeo$ ) and type-0 ( $eee$ ) frequency doubling processes. In the low depletion limit the dominant feature of this system is the effect of the relative phases of the fundamental components,

which influence the second harmonic output by their mixing in Eq. (4). However, for the case where an appreciable efficiency is achieved and depletion of the fundamental is significant, energy exchange between the fundamental components and nonlinear phase-shifts from cascading can occur. The temperature detuning curves for the system of Eqs. (2)-(4) were simulated numerically for congruent lithium niobate, again using Sellmeier equations from [11]. To reflect the temperature dependence of the wave vector mismatches we express them as:

$$\Delta k_1(T) = \Delta k_{oe}(T) - G_1, \quad (5)$$

$$\Delta k_0(T) = \Delta k_{ee}(T) - G_7. \quad (6)$$

In Eqs. (5) and (6)  $G_1$  and  $G_7$  are the 1<sup>st</sup> and 7<sup>th</sup> order reciprocal QPM lattice vector values for the designed poling period, and are assumed to be constant over the temperature bandwidth of the phase-matching curves. A crystal length of 4.5 mm, similar to that fabricated for the experiments was simulated, and the nonlinear constants were set to be equal, approximately corresponding to the regime described by Eq. (1). The simulation was initially conducted with sufficiently large amplitudes to produce ~30% second harmonic conversion from both fundamentals, making for convenient viewing of all fields on the same scale. The irradiances have been normalized with respect to half of the total fundamental irradiance, which is being shared equally between the two orthogonal components ( $I_{total}/2$ ).

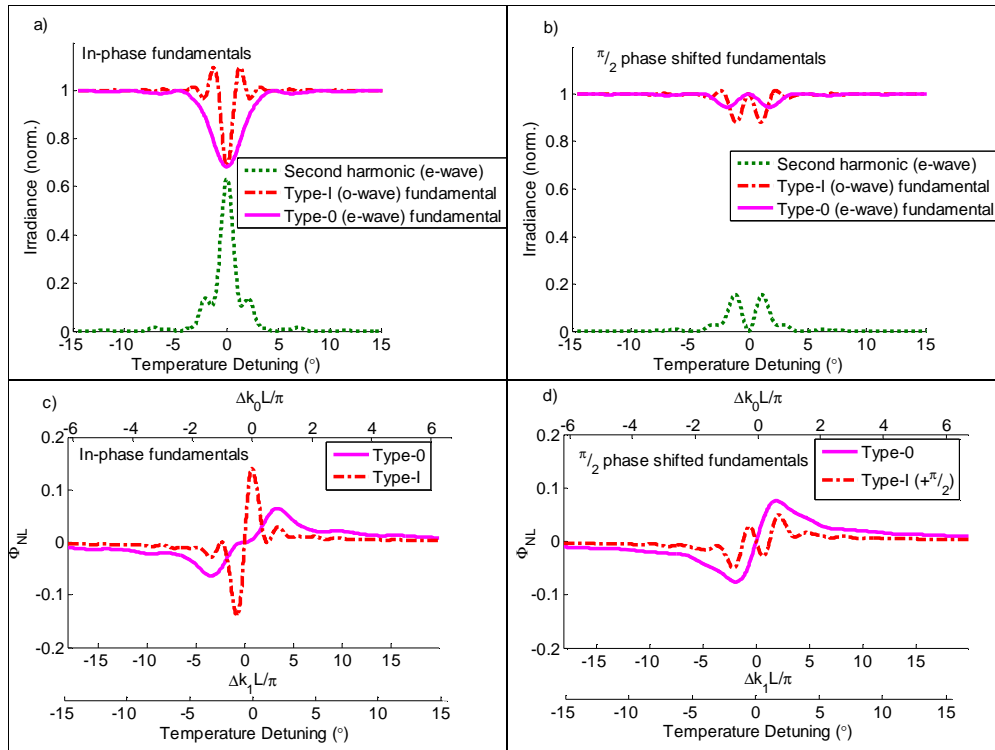


Fig. 3. Temperature detuning curves for SHG, and nonlinear phase-shifts of fundamentals for simultaneously phase-matched type-0 and type-I SHG in 4.5 mm long lithium niobate. Plots a) and b) show the calculated SHG detuning curves for fundamentals launched in-phase and with a  $\pi/2$  phase shift respectively. Plots c) and d) show the calculated nonlinear phase shift of the fundamental fields fundamentals launched in-phase and with a  $\pi/2$  phase shift respectively.

A feature of this system is that the temperature acceptance bandwidths of the type-0 and type-I phase matchings in lithium niobate are appreciably different, which results in various degrees of interplay between the two processes across the detuning range. In the plots on the left of Fig. 3, we see the case for in-phase fundamentals. The detuning curve for the SH is representative of the superposition of the two individual processes with differing bandwidths, which would individually have  $\text{sinc}^2$  detuning functions. For the narrower-temperature-bandwidth, type-I fundamental, energy exchange from the SH field produced by the broader-band type-0 phase matching can be seen. This is accompanied by an enhanced nonlinear phase-shift of the type-I fundamental at detunings of  $\Delta k_1 L \approx \pm\pi$ , as shown in the lower left plot of Fig. 3. This is due to a larger SH field being available, produced by the broader-band type-0 SHG, compared to that of a single SHG process. This contributes to the back-conversion and phase-shifting of the narrower-band type-I fundamental. When the fundamentals are launched phase shifted by  $\pi/2$  with respect to each other, as shown in the right of Fig. 3, they interfere destructively at zero detuning suppressing any SHG and energy exchange. At slight detuning we see some slight back conversion, but due to the suppressed SH field this is small compared to the in-phase case, and the nonlinear phase-shift while, changing in a different manner across the detuning, is of much lower magnitude. The  $\pi/2$  phase shifted case is however useful for inducing parametric back conversion for the case where the magnitudes of the fundamental components are different. In this case the stronger fundamental prevails and energy from the strong fundamental couples into the weaker fundamental via the second harmonic field. This is facilitated by the weaker fundamental being in-phase with the SH field allowing for difference frequency mixing. Shown on the left of Fig. 4 is the case for fundamental components launched with power ratio of 7:3 (*e:o*). We see the weaker *o*-wave experiences an increase in power at zero detuning. Shown on the right of Fig. 4 is the relative gain of the *o*-wave at zero detuning ( $\Delta k=0$ ) for a variety of ratios of the fundamental power in the *o* and *e* components, but for a fixed net power (equivalent to a value of 2 in the above graphs). This is shown for a variety of nonlinear efficiencies of the parent SHG processes, which in practice is explored by using longer crystals, higher laser peak power or higher material nonlinearities. These simulated results are presented in this fashion so as to correspond to our experimental case, where the ratio of power in the orthogonal polarization components was controlled by rotating a half-wave-plate with respect the crystal axes.

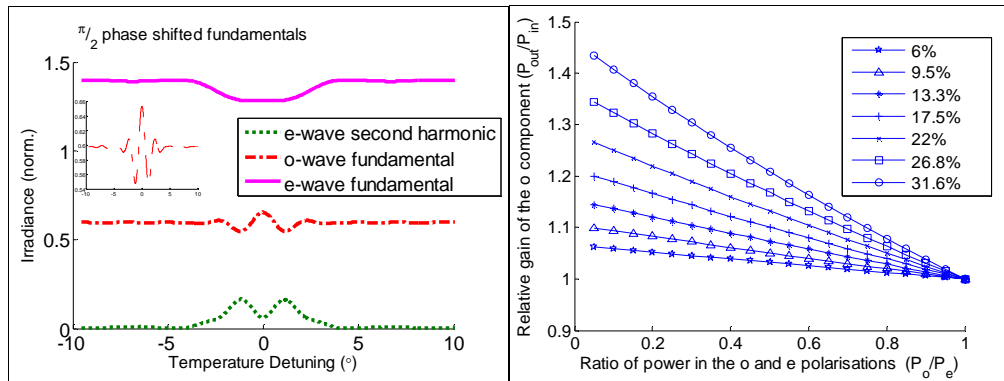


Fig. 4. Left: cascading of energy from a dominant e-wave fundamental field to a weaker o-wave fundamental field when the two fundamentals are launched with  $\pi/2$  phase shift. Inset shows rescaled plot for o-component demonstrating parametric gain at zero detuning. Right: relative parametric gains of the *o*-polarized component (involved in type-I SHG) in relation to the ratio of *o-e* polarizations plotted for various efficiencies of the parent SHG processes.

#### 4. Experiment

The experimental setup is shown in Fig. 5. The laser source was a lab-built Q-switched Nd:Gd:YVO<sub>4</sub> laser operating on the 1064.5 nm line with a 10 kHz repetition rate, 20 ns pulses

and ~1 kW peak power. Wave-plates were used to control the laser polarization, and a Glan prism was used to resolve the polarization components after frequency conversion in the PPLN. The quarter-wave-plate was inserted when  $\pi/2$  phase shift between the two fundamental components was investigated, and was aligned on the axes of the lithium niobate sample. The half-wave-plate was used to control the relative magnitudes of the two fundamental components. For low power measurements at the fundamental wavelength, a Pellin-Brocca prism was used to separate the second harmonic. Calorimetric power meters and photo diodes were used to monitor the average output power and pulse shapes respectively.

Coincident phase-matching of the individual type-0 and type-I SHG is shown in the temperature detuning curves in Fig 6. Overlap of these curves is very sensitive to the period presented by the crystal and thus rotation of the crystal results in off-setting the curves, changing the  $\Delta k$ 's of the two processes relative to each other. In this way the crystal angle can be used to control the relative phase-mismatch between the two processes. Figure 6 shows that the temperature detunings closely resemble the expected  $\text{sinc}^2$  relations, and the two phase-matchings exhibit very similar peak efficiencies, allowing for a robust comparison with the numerical simulations above.

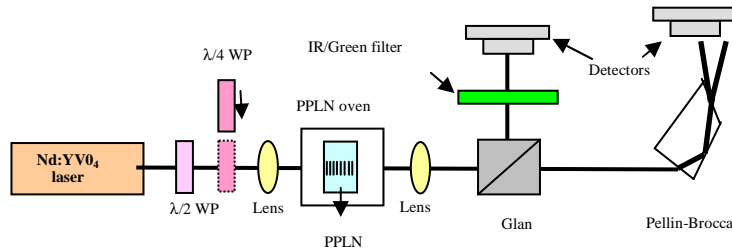


Fig. 5. Experimental layout for investigating simultaneous phase-matching and  $\chi^{(2)}:\chi^{(2)}$  cascading in single period PPLN using a Nd:Gd:YVO<sub>4</sub> as the source. (WP' – waveplate.)

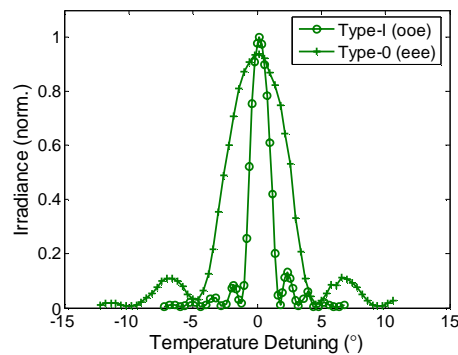


Fig. 6. Temperature detuning curves for type-I (1<sup>st</sup> order QPM on  $d_{31}$ ) and type-0 (7<sup>th</sup> order QPM on  $d_{33}$ ) SHG of a 1064.5 nm laser in 45.75  $\mu\text{m}$  period PPLN. Each curve is measured separately with either a pure type-0 or type-I polarization being set as the input. Irradiance has been normalized to peak SH irradiance of the type I process.

## 5. Results

Simultaneous phase-matching of the two SHG processes was investigated by setting the laser polarization to 45° with respect the crystal axes so that the o and e components were of equal magnitude. The QWP was inserted for the case of  $\lambda/2$  phase shift between the two fundamental components as described above. The results for the in-phase case are shown in



Fig. 7. The fundamental detuning curves indicated a peak conversion efficiency approaching 6% for each process, and the simulation was adjusted for similarly direct comparison. The measured detuning of the SH shows excellent agreement with the simulation, confirming simultaneous action and cross-talk between the two processes. The measurements for the fundamental components were complicated by oscillations in the polarizations due to the slight wave-plate (changing birefringence) action of the lithium niobate crystal as the temperature is changed, but still maintain good quantitative agreement with the simulation. Most notably the increase in the narrow-band type-I fundamental near zero detuning was clearly seen confirming the presence of cascading between the two processes. The case where a  $\pi/2$  phase shift was introduced between the two fundamentals is shown in Fig 8. The measurements again show quantitative agreement with the simulations. The discrepancy present in the SHG detuning curve may be indicative of the slight difference in efficiency of the two processes as indicated by Fig 6. However the strong suppression of the SH and zero depletion of the fundamentals at zero detuning is again indicative of the simultaneous action and crosstalk of the two processes.

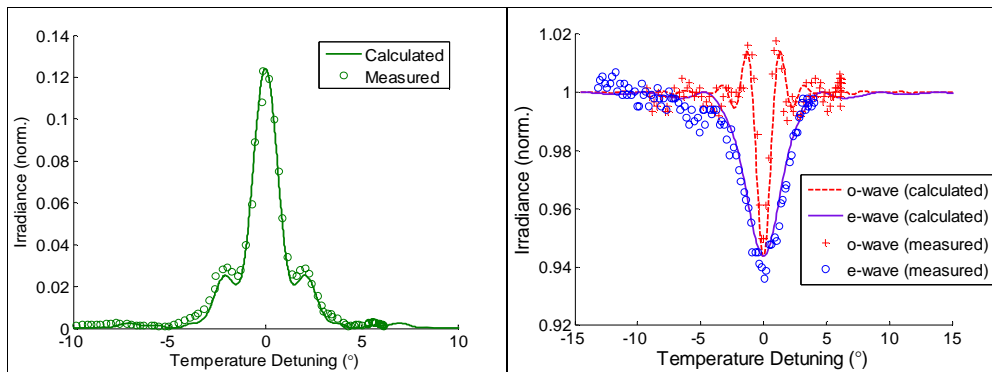


Fig. 7. Temperature detuning curves for simultaneous type-I and type-0 SHG from equally intensive and in-phase fundamentals. Left: measured and calculated detuning curve for the SH. Right measured and calculated detuning curves for the o-wave fundamental and e-wave fundamental.

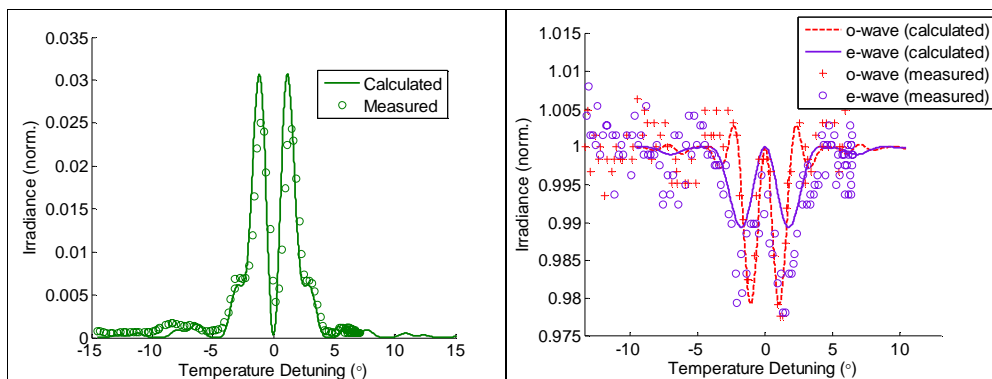


Fig. 8. Temperature detuning curves for simultaneous type-I and type-0 SHG processes. The two o- and e- fundamentals are with equal intensities and  $\pi/2$  phase shifted. Left: measured and calculated detuning curve for the second-harmonic wave. Right: measured and calculated detuning curves for the o- and e- fundamental waves.

Back-conversion in the case of  $\pi/2$  phase shifted fundamentals with different magnitudes was investigated by using the HWP to change the ratio of the  $e:o$  polarization components, while leaving the QWP aligned on the crystal axes to maintain a  $90^\circ$  phase between them.



Rather than displaying zero depletion at zero-tuning, as is the case for equal magnitudes, the weaker polarization component experiences parametric gain as a consequence of cascading. This was measured for the type-I fundamental (o-polarized) for various ratios of the e-o magnitudes ranging from 1:1 to 95:5. The detuning data for the case of a 7:3 ratio (*e:o*) is shown on the right of Fig. 9 and shows a good agreement with our numerical simulations. The peak relative parametric gain for various ratios of fundamental components is shown on the right, along with the calculated relation for the case of 6% SH efficiency shown in Fig. 4.

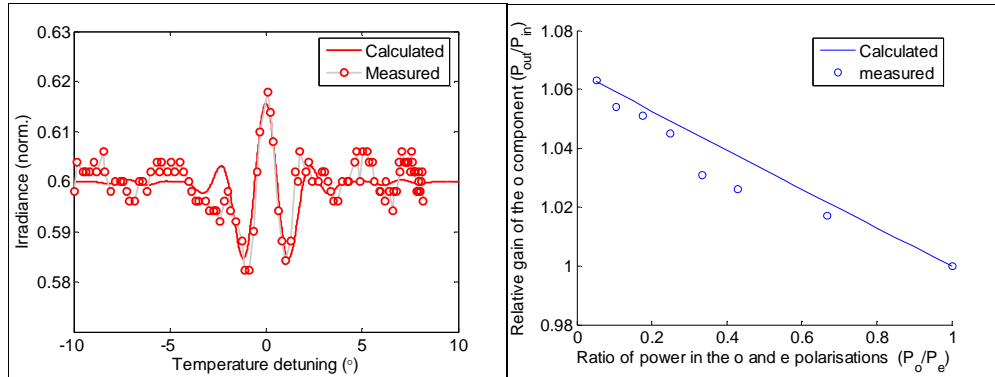


Fig. 9. Left: detuning curve for the weaker type-I (o-polarized) fundamental component when the ratio is 3:7 (o:e) and it is phase shifted with respect to the other type-0 (e-polarized) fundamental. Left: relative parametric gain of the type-I (o-polarized) fundamental in relation to the ratio of the magnitudes of the fundamental components.

## 6. Discussions

A more device orientated presentation of the parametric amplification is a pump-signal regime (rather than the changing ratios with wave-plates presented in our proof of principle results here) where a constant power “local” pump is present in the crystal and the transfer function of the signal light of varying magnitude is of interest. Figure 10 shows simulations of the net fractional gains and transfer functions of a signal experiencing parametric gain for various levels of efficiency of the pumps starting SHG without signal present. The signals peak net gain increases with the efficiency of the nonlinear processes as more second harmonic (SH) is available to facilitate cascading. All efficiencies exhibit similar traits of providing low net gain to small magnitude signals, maximum gain for mid range magnitudes and lower net gain for high range signal magnitudes, returning to zero net gain as the signal approaches the pump level and perfect interference takes place. The corresponding transfer functions are shown on the right of Fig. 10, and they are plotted with the signal magnitude going beyond that of the pump. For signal magnitudes beyond that of the pump, the transmission of the signal flattens off, especially for the high efficiency cases, as it is now the dominant field and sees depletion into the SH wave. Such traits may be useful for improving signal-noise ratios, and also for normalizing pulse train amplitudes, however drastic improvements in the nonlinearity considered here need to be made before application to communication type powers is considered. Waveguides of many varieties are readily implemented in lithium niobate and are often used to improve the nonlinear efficiency and make devices compatible with fiber based systems, however engineering the waveguide properties to ensure that both polarizations are phase-matched simultaneously and share good modal overlap with the second-harmonic may be challenging. Longer sections of PPLN, typically 10 times the length of that reported here, are commercially available and would greatly improve the efficiency. However the challenge of overlapping two orthogonal processes, both in wavelength and temperature, in long crystals where the detuning bandwidths are much narrower presents a challenge to the fabrication process, as well as the fact that higher order QPM, as implemented in our case, is extremely sensitive to fabrication errors such as duty cycle variations and local periodicity fluctuations.

Applying chirp and apodization to the QPM grating to ensure a reasonable bandwidth for short pulse lasers and broadband devices may also complicate this particular implementation's use of higher order QPM. Other solutions to the problems of the PM curves narrowing for long samples, and the doubling of large wavelength bandwidths, have recently been suggested. One example of such approach is the recently published method of using short range order in a pseudo-random 2D array [18] which provides broadband QPM.

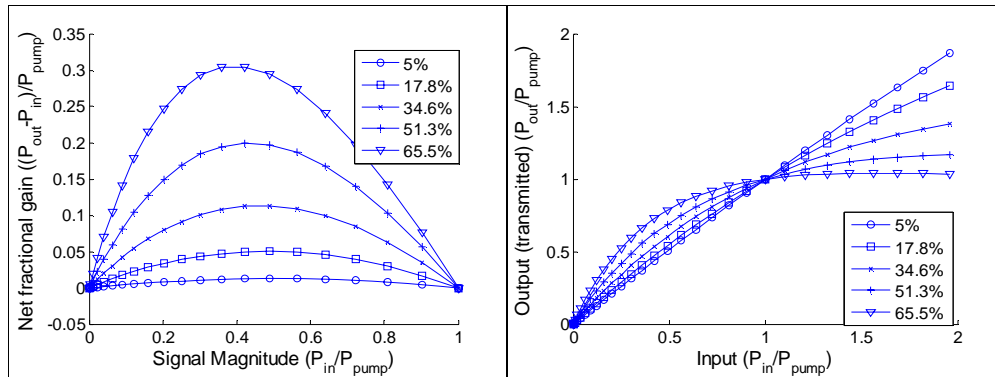


Fig. 10. Left: Net fractional gains in relation to signal magnitudes for a variety of pump levels with shown SH efficiency. Right: Transfer function of signals for a variety of pump intensities with shown SH efficiency.

## 7. Conclusions

We have reported on experimental studies of the cross-talk interaction between two cross-polarized fundamental waves under condition where each fundamental wave is involved in two separate phase-matched SHG processes but with a common second-harmonic wave. The energy exchange between the two fundamental waves can be observed when the two SHG processes are simultaneously phase matched and the input fundamental waves have enough intensity to ensure at least 10% SHG efficiency with respect to the total input energy. The effect has been compared with the dependences obtained from the developed numerical calculations. The observed good agreement demonstrates that numerical simulations of the coupled-field equations accurately describe this special type of two-color cascading process. We expect the same effect will be even more easily observed with short (picosecond or femtosecond) pulses, with an additional consideration that the crystal length be chosen so that the effects due to group-velocity mismatch between *o* and *e* polarizations do not become an overriding factor. The advantage of the proposed interaction is its instantaneous character due to the nonlinearities involved being of the second order. Similar schemes for the parametric energy exchange are possible due to two beam coupling [19] with involvement of the photorefractive effect, but the energy transfer in this case is of a much slower time scale.

## Acknowledgments

This work has been supported by the Australian Research Council under the Centers of Excellence program and the Discovery Fellowship scheme.